

Simple measures to capture the robustness and the plasticity of soil microbial communities

Takashi Shimada

*Department of Systems Innovation, School of Engineering, The University of Tokyo and
Mathematics and Informatics Center, The University of Tokyo*

Kazumori Mise

*Graduate School of Agricultural and Life Sciences, The University of Tokyo
Graduate School of Science, The University of Tokyo and
Bioproduction Research Institute, National Institute of Advanced Industrial Science and Technology*

Kai Morino

Interdisciplinary Graduate School of Engineering Sciences, Kyushu University

Shigeto Otsuka

*Graduate School of Agricultural and Life Sciences, The University of Tokyo and
Collaborative Research Institute for Innovative Microbiology, The University of Tokyo*

(Dated: September 6, 2024)

Soil microbial communities are known to be robust against perturbations such as nutrition inputs, which appears as an obstacle for the soil improvement. On the other hand, its adaptable aspect has been also reported. Here we propose simple measures for these seemingly contradicting features of soil microbial communities, robustness and plasticity, based on the distribution of the populations. The first measure is the similarity in the population balance, i.e. the shape of the distribution function, which is found to show resilience against the nutrition inputs. The other is the similarity in the composition of the species measured by the rank order of the population, which shows an adaptable response during the population balance is recovering. These results clearly show that the soil microbial system is robust (or, homeostatic) in its population balance, while the composition of the species is rather plastic and adaptable.

Understanding of the stability of ecosystems has been a central question in ecology, often with emphasis on local stability, persistence, permanence, resilience, etc., and its relation to its diversity [1–13]. It has also been inspiring broader field to consider the robustness of complex systems which consist of many components interacting each other more in general [14–22]. However, empirical tests of various theoretical predictions on animal-plant ecosystems have been limited within natural experiment, i.e. comparing the systems under different environment and with different history. This is mainly due to the large scales in space and time scale, for conducting controlled experiments.

Microbial ecosystems are one of the best systems to resolve such situation, because they are easy to manipulate and their development can be observed in a shorter time scale. Bacteria in soil are also known to be extremely abundant and diverse, with estimates generally ranging from 10^6 to 10^{10} cells [23] and 6,400 – 38,000 taxa [24] per gram of soil. These bacteria play vital roles in biogeochemical cycling, plant growth, and the maintenance of terrestrial ecosystems. Reflecting the importance of soil functions for terrestrial ecosystems, there has been considerable effort invested in understanding the response of soil ecosystems to disturbance [25]. The possibility of such approach was brilliantly illustrated in a pioneering work on the microbial communities of natural soil and natural water [26]. In that study, it was shown that the macroscopic characteristics of the micro-ecosystems such as those dry weight and pH can be modulated by an artificial natural selection process. And the difference was inherited to the following systems even after quitting the natural selection. This shows that the microbial ecosystem have both plasticity and robustness or stability in macroscopic sense, while the underlying microscopic mechanism remained largely unknown.

Advance of DNA sequencing technology has enabled microbiologists to obtain detailed information on dozens of microbial communities at one time [27, 28]. This has paved a way to elaborate time-series investigation of microbial ecosystem successions [29, 30]. While many have elucidated the succession of microbial communities in a descriptive manner, for example by cataloguing a plethora of microbial clades (taxonomic groups) that increase or decrease during the ecosystem development [31, 32], others summarize the dynamics of the systems using statistical features such as co-occurrence network indicators or ARIMA modeling [30, 33]. Other characteristics such as the shape of species abundance distribution [34] and the network structures of interactions [35] have been also the target of investigation. However, the interpretation of these features is by no means straightforward.

In this study, we propose simple and comprehensible measures to characterize the state of microbial communities, based on the balance and the composition of populations of the operational taxonomic units (OTUs). These two measures are independent each other in the sense that there always exists a direction to modulate the community so

that one measure changes while the other is kept constant. It is shown that these measures well capture the conserved aspect (relating to the stability, robustness, etc.) and the adaptive aspect (plasticity) of the microbial community.

RESULTS

System and Preparation

As a model system of community dynamics in response to perturbation, we here use time-series data of soil microbial communities receiving nutrient input [36]. This dataset consists of soil microbial community structures (populations of OTUs) at five time points, i.e. 0, 3, 10, 17 and 24 days after initial preparation. As shown in TABLE I, the nutrient input condition consists of the combination of nitrogen source: ammonium chloride (NH_4Cl , denoted by A in the labeling of the conditions) or urea (U), carbon source: glucose (G) or cellobiose (C). We also have two types of input schedule: either once in the beginning of the observation (day 0) or addition of one quarter of the amount four times every week (days 0, 7, 14, and 24), denoted by 1 and 4 in the labeling of the condition, respectively. Negative controls without nutrient input were also prepared (“Control”).

This nutrient amendment schemes were designed to cover various intensities and types of perturbations. Urea and cellobiose represent more slowly acting nutrition sources than ammonium and glucose, since the former two require enzymatic degradation before being catabolized by microbes. Regarding the input schedules, the one-time and the four-time schemes represent large abrupt perturbation and small but continuous perturbation, respectively.

Since we have three samples for each condition, a soil sample α is specified by the combination of all these parameters as: $\alpha = (t, d, s)$, where $n \in \{\text{Control, AG1, AG4, AC1, AC4, UG1, UG4, UC1, UC4}\}$, $d \in \{0, 3, 10, 17, 24\}$, and $s \in \{1, 2, 3\}$ represent the treatment condition, observation day, and the sample number for each condition, respectively. Because the data $d = 0$ is only for Control, the total number of the soil samples is $(1 \times 5 \times 3) + (8 \times 4 \times 3) = 111$.

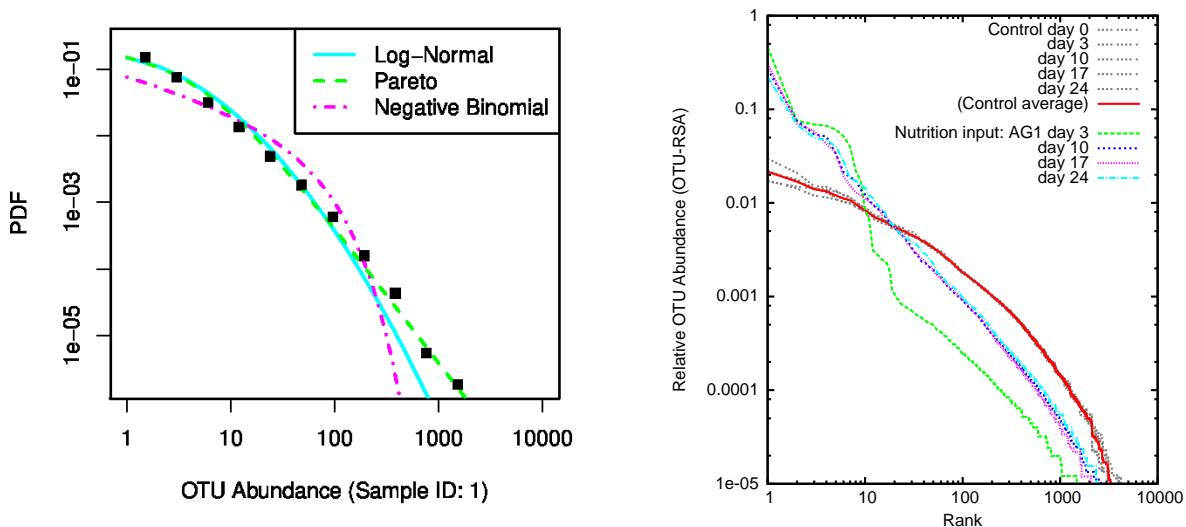


FIG. 1. (Left) An example of the probability distribution function of OTU abundance of soils before nutrition inputs (“control”, sample ID 1). The distribution is well fit by log-normal distribution and Pareto distribution. (Right) Rank-size plots of relative OTU abundances (OTU-RSA) of control soils and that of a soils after a one-shot nutrition input (AG1) in log-log scale. While OTU-RSA shape is well kept among control soils, OTU-RSA of the soils after the perturbation are deformed significantly which is characterized by the enhanced dominance of top ~ 10 OTUs. OTU-RSAs in the later time stage relax to a smoother distribution, which is similar to the original shape.

TABLE I. The nutrient input patterns in the data set of microbial community experiment, together with the basic characteristics of the soils under those conditions in the earliest (3days) and latest (24 days) time. The population-balance-based similarity \mathcal{B} and the OTU composition-based similarity \mathcal{C} to the average of control communities are also shown. The diversity and the dominance here represent the Shannon entropy of RSA: $S_\alpha = \sum_r -p_\alpha(r) \ln p_\alpha(r)$ and the proportion of the sum of the abundances of top 10 OTUs to the total abundance, respectively. $\bar{\mathcal{B}}^{NB}$ and $\bar{\mathcal{C}}^{NC}$ are the averages of the proposed similarity to the control samples in the population balance and in the OTU composition which are defined as Eq. (2) and as Eq. (4), respectively.

t (treatment)	Condition				Characteristics						
	Nitrogen	Carbon	Timing	d (obs. day)	Diversity S	Dominance	#OTU	$\bar{\mathcal{B}}^{1000}$	$\bar{\mathcal{C}}^{30}$	$\bar{\mathcal{C}}^{100}$	$\bar{\mathcal{C}}^{300}$
Control	none	none	-	3	6.648	0.146	3805	0.969	0.804	0.790	0.749
				24	6.823	0.112	4324	0.985	0.844	0.824	0.773
AG1	NH ₄ Cl	Glucose	First Day	3	2.588	0.875	1696	0.580	0.258	0.332	0.437
				24	4.649	0.522	2861	0.708	0.175	0.064	0.257
AG4	NH ₄ Cl	Glucose	Weekly $\times 4$	3	4.032	0.625	3162	0.568	0.351	0.436	0.542
				24	4.655	0.526	2906	0.737	0.104	0.155	0.310
AC1	NH ₄ Cl	Cellobiose	First Day	3	2.678	0.864	1867	0.601	0.230	0.349	0.428
				24	4.429	0.543	2462	0.726	0.070	0.008	0.220
AC4	NH ₄ Cl	Cellobiose	Weekly $\times 4$	3	4.073	0.634	2897	0.592	0.353	0.494	0.588
				24	5.012	0.433	3032	0.737	-0.017	0.003	0.218
UG1	Urea	Glucose	First Day	3	3.302	0.774	2034	0.644	0.159	0.295	0.424
				24	4.681	0.503	2668	0.736	0.085	0.058	0.227
UG4	Urea	Glucose	Weekly $\times 4$	3	3.792	0.682	2652	0.584	0.347	0.517	0.575
				24	5.155	0.407	2730	0.779	0.101	0.018	0.181
UC1	Urea	Cellobiose	First Day	3	3.615	0.737	2325	0.650	0.174	0.340	0.433
				24	4.958	0.434	2621	0.846	-0.016	-0.161	0.121
UC4	Urea	Cellobiose	Weekly $\times 4$	3	0.546	3.460	2582	0.560	0.295	0.501	0.547
				24	0.690	4.828	2612	0.698	0.017	0.007	0.182

Species Abundance Distributions

We first confirm the basic characters of the control communities by its relative abundance distribution (RSA) of operational taxonomy units (OTU), which we shall call OTU-RSA. For this purpose, we compare the fittings by classical theoretical distributions for species abundance of ecological systems, namely, log-normal distribution, power-law (Zipf/Pareto) distribution, and the negative binomial distribution. An example of fitting is shown in the left panel of Fig. 1. OTU-RSA of control soils are found to be better fit by log-normal distribution and power law distributions than by the negative binomial distribution, with a distinctive difference in the log-likelihood and equivalently in AIC, since all these distributions have two parameters. The obtained fitting parameter values consistently indicate that the OTU-RSA of the soil microbe ecosystem before any disturbance is broad (see Materials and Methods and SI for detail). This feature is consistent with the systems under natural environment[34], implying that the control soils are keeping such an intact state.

The abundance distributions of the soils under or after nutrition input are also fat-tailed, with typically narrower shape comparing to that of control soils (Fig. 1, right panel). A typical response of RSA to the nutrition input is characterized by an initial decrease of diversity which is measured by the number of detectable OTUs or by Shannon entropy of OTU abundances

$$S = - \sum_r p(r) \ln p(r), \quad (1)$$

and an increase of the dominance of top tens of OTUs. This decrease is followed by the recovery to a smoother distribution which is nearer to that of original control soils (TABLE I and Supplemental Information). Such changes in RSA clearly illustrates a homeostatic aspect of the soil microbial ecosystem: Fertilization typically first leads

to more oligopolistic abundance distribution but the system later shows a resilience toward the original population balance.

Similarity in RSA shape

The above observation about the typical change in the shape of OTU-RSAs naturally motivates us to define a similarity measure solely based on that. A simple and natural choice is to take the linear correlation coefficient between the relative OTU abundances of soil α and soil β in the same rank r ,

$$\mathcal{B}_{\alpha\beta}^{R_B} \equiv \frac{\sum_{r=1}^{R_B} (p_r^\alpha - \bar{p}^\alpha) (p_r^\beta - \bar{p}^\beta)}{\sqrt{\sum_{r=1}^{R_B} (p_r^\alpha - \bar{p}^\alpha)^2} \sqrt{\sum_{r=1}^{R_B} (p_r^\beta - \bar{p}^\beta)^2}}, \quad (2)$$

where p_r^χ represents the relative abundance of the OTU whose abundance rank is r in soil χ , and $\bar{p}^\chi = \sum_{r=1}^{R_B} p_r^\chi / R_B$ denotes the average abundance up to the maximum rank R_B to be taken into account. Since OTU-RSA has broad shape, the maximum rank R_B in the following will be set at 1,000 to include the information from as diverse OTUs as possible.

The average \mathcal{B} similarities of the soil communities under each treatment condition t observed on day d to the control soil,

$$\bar{\mathcal{B}}(t, d) = \frac{\sum_{t_\alpha=t, d_\alpha=d; t_\beta=\text{Control}} \mathcal{B}_{\alpha\beta}}{\sum_{t_\alpha=t, d_\alpha=d; t_\beta=\text{Control}} 1}, \quad (3)$$

are shown in Fig. 2 (bars). We can see that the temporal evolutions of the soils in this measure against various inputs (different combinations of nutrition and the different schedules) universally show a homeostatic response, i.e. the similarity to the original control community first drops and that recovers later on. The response of the soils against the continuous inputs is particularly interesting, because the recovery takes place during the successive nutrition input. This is why we regard it homeostatic, rather than a mere relaxation back to the original state under absence of the perturbation.

Similarity in OTU abundance rank orders

We next seek a measure to capture a totally different aspect of the soil microbial community. Because the systems have been confirmed to show robustness in its population *balance* (the shape of RSA), the remaining degree of freedom in OTU abundance distribution is in its *composition*. Suppose that two communities have the same OTU-RSA, then yet two communities can be different if OTUs occupying each rank position are different each other. In other words, the order of OTUs in relative abundance (whether a particular OTU is major to another particular OTU) is independent of the shape of OTU-RSA distribution.

Our similarity measure for the composition of OTUs, with respect to the OTU-RSA information, is defined by the Kendall's rank correlation between the abundance ranks of top N_C major OTUs of the two communities in comparison, α and β :

$$\mathcal{C}_{\alpha\beta}^{N_C} \equiv \frac{\#_c - \#_d}{N_C(N_C - 1)/2}, \quad (4)$$

where $\#_c$ and $\#_d$ represent the numbers of concordant OTU rank pairs, i.e. $(r_i^\alpha - r_j^\alpha)(r_i^\beta - r_j^\beta) > 0$, and discordant OTU rank pairs, i.e. $(r_i^\alpha - r_j^\alpha)(r_i^\beta - r_j^\beta) < 0$, respectively. Where r_k^χ represents the abundance rank of OTU k in the soil χ . If a certain OTU is not detected in the sample, we replace r_k^χ by a uniform number r_{\max} which is larger than the total number of OTUs. Therefore, for example, if both OTUs i and j are missing in a soil α , any combination of OTU abundance ranks in the other soil β (r_i^β and r_j^β) will not be counted as concordant or discordant. The

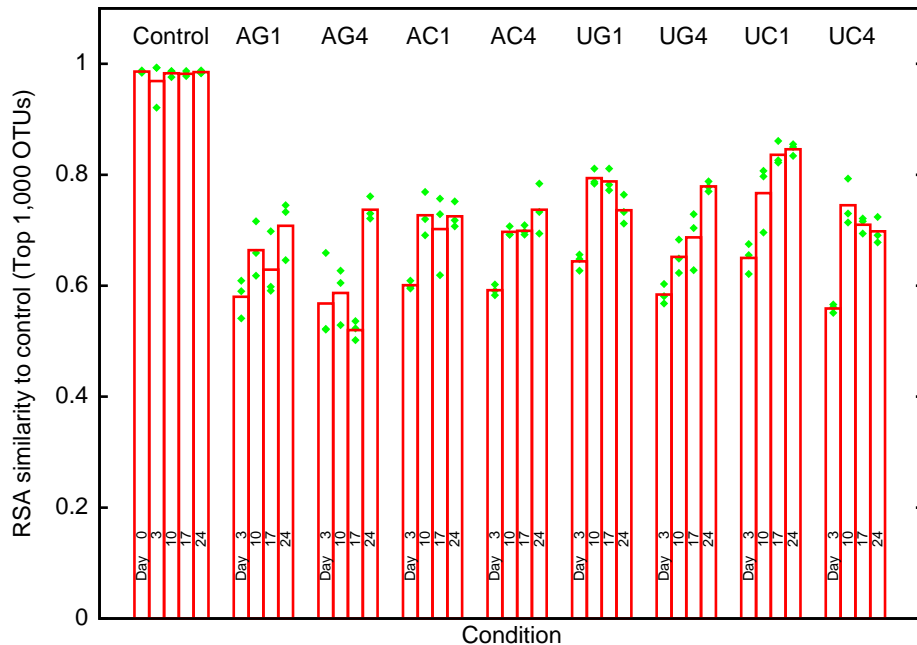


FIG. 2. Similarities of the soil communities under the various conditions measured by the RSA-shape-based metric \mathcal{B} , against the communities of control soils. Bars represent the average similarity of the samples under each treatment condition t and the observation day d to the control soils and the points represent the average similarity of each sample to the control soils. While the control samples keep high similarity over time, \mathcal{B} of the communities after the pulsive nutrition inputs show sharp drop and that is followed by partial recovery in the later time. The similar dynamics of drop and recovery is observed also under successive nutrition inputs.

parameter N_C is chosen to be large enough to take as much information as possible and not too large to avoid an error from the detection limit. To determine proper N_C , we first check how many OTUs are commonly observed in the soils under different conditions. For this purpose, we evaluate the overall popularity (majority) of each OTU by aggregating the all OTU abundances across the available conditions. We find that almost all of top 300 major OTUs in the aggregated data are found to be shared in all soils (shown in SI, Fig. S-2). Some of the OTUs in the following overall majority rank range becomes to be absent (undetectable) in some soils. Therefore, in the following we choose $N_C = 100$, OTUs up to this are expected to provide the majority-minority information well above the detection limit of OTU abundances in the current experiment. One can confirm that the following results are not sensitive to the precise choice of N_C (for example, for $N_C = 30$ and $N_C = 300$).

The present measure \mathcal{C} takes 1 if the rank orders between OTUs (major-minority relations) is kept for all pairs, and it takes a value near 0 if there is no correlation. It can take negative value if the reversal in the majority order is dominant, ultimately down to -1 when all the majority order pair are flipped. Because this measure is independent of the shape of RSA distribution, and also because the swap in the ordering of OTU abundances does not change the RSA shape, the previously defined “population-balance measure” \mathcal{B} and the currently introduced “composition measure” \mathcal{C} can be said to be independent, or *orthogonal*, to each other.

The OTU composition similarities \mathcal{C} measured using the top $N_C = 100$ major OTUs are shown in Fig.3, where bars again represent the average similarity of the samples with treatment condition t and the observation day d to the control soils:

$$\bar{\mathcal{C}}(t, d) = \frac{\sum_{t_\alpha=t, d_\alpha=d; t_\beta=\text{Control}} \mathcal{C}_{\alpha\beta}}{\sum_{t_\alpha=t, d_\alpha=d; t_\beta=\text{Control}} 1}. \quad (5)$$

The similarity among the control soil is confirmed to be high in this metric. Compared to that, the average similarities of the soils 3 days after nutrition inputs to the control soil is low, meaning that the composition of OTUs are changed greatly from the control soils. What is remarkable is that the similarity of the perturbed soils to the control soils

shows further decrease in the later time. This tendency is universally observed for different conditions, and for the choice of N_C as shown in the Table I and SI. Recalling that the \mathcal{B} similarity shows an increase in the same moment of later time stage, the observed further change in OTU composition takes place during the recovery process of the population balance. This implies that the response in the composition measure \mathcal{C} is not just due to a slower response, but is capturing the plasticity of the soil community to the nutrition input.

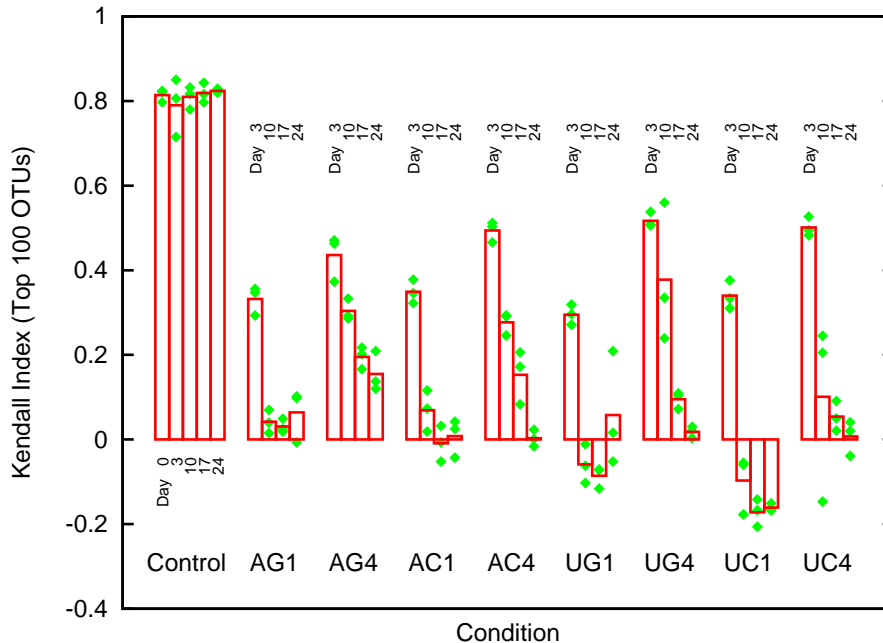


FIG. 3. OTU composition similarities \mathcal{C} to the control soils. Each bar represents the sample average of the soils under each perturbation condition and timing, with the similarity of each soil is shown with the symbols (three samples for each condition). Compared to the high similarity among control conditions, \mathcal{C} similarities after first fertilization (Day 3) are lower. And the similarities show further decrease in the later time, even for the pulsive input, i.e. during the period without any further input.

DISCUSSION

In this study, we have proposed simple similarity measures to characterize the response of the soil microbial communities to nutrition inputs. The first one, \mathcal{B} , is based on the *balance* of the populations (shape of OTU-RSA), and the other one, \mathcal{C} , is based on the *composition* of OTUs. The both similarities among the control soil communities are kept during our observation time of 24 days, meaning that the stationary character of the communities under no external inputs is well captured by these macroscopic measures.

When the nutrition inputs are applied, the immediate response of the communities appears as the significant drops in both similarities. The typical temporal evolutions of the similarities in the later time are, however, different each other. The \mathcal{B} similarities of the perturbed soils to the original communities universally show a recovery in time. The recovery is observed even under the continuous nutrition input. Therefore this measure universally characterizes the robust (or homeostatic) nature of the soil communities. In \mathcal{C} , on the other hand, an opposite character of the soil's response is detected. The \mathcal{C} of the perturbed soils generally show further decrease in time, in the middle of the recovery period in \mathcal{B} similarity (10, 17, and 24 days after the onset of nutrition inputs). This further decrease is universal among different nutrients and input schedule, while the continuous input tends to results in more monotonic decay. Therefore the plastic (or adaptive) aspect of the soil communities is also well captured by the \mathcal{C} similarity.

Most of the attempts which have so far been made to disentangle the dynamics of complex microbial community structures rely on beta-diversity metrics between spatially/temporally distant communities. The concept of beta-diversity appears to be two-fold. While it was originally proposed as a between-community difference in the presence/absence of each species [37], currently popular metrics such as Bray-Curtis [38] and weighted UniFrac distances [39] bear the information on the quantitative balances between community members. The two indices we have proposed here are approximately congruent with these beta-diversity-based distances, in the sense that both \mathcal{B} and \mathcal{C}

are reflected. This can be seen in the present data that the drastic changes the soil bacterial communities underwent after the initial perturbations (i.e. between days 0 and 3) is visible by the beta-diversity measures (Fig. S-1 in SI). However, in these measures, the rapid recovery in species balances (i.e. change in \mathcal{B}) has overwhelmed and masked the long-lasting effect on the change in microbial community members (i.e. change in \mathcal{C}). It is also notable that the contrast between two schemes of nutritional input schedule, one-time and four times, are obscure in \mathcal{B} (and in canonical beta-diversity) but clearly highlighted by \mathcal{C} . Therefore, by decomposing the canonical beta-diversities into two features by \mathcal{B} and \mathcal{C} , otherwise mingled differences between incubation conditions are better illuminated.

For the understandings of the robustness and plasticity of interacting communities in more general sense, present discovery can be regarded as a good guiding principle. Let us consider trying the construction of a dynamical community model, under a constraint that which can explain the coexistence of observed robustness and plasticity. As is evident from the large change in OTU-RSA shape, the homeostatic response to the nutrition input we have observed by \mathcal{B} is beyond linear (local) stability argument. Therefore, the observed trajectory should be explained as a transition from an attractor (a stable state) to another attractor triggered by the change of nutrition parameter or a large disturbance in population distribution. A challenge in such approach is that one should reproduce the order of the response: the recovery in OTU balance takes place first and the dynamics of the OTU composition change is slower. Another possibility to explain the robustness in OTU-RSA, with keeping the degree of freedom of change in the OTU composition, would be a more statistical (entropic) mechanism under some hidden microbial constraints. The neutral theory is a good candidate for this, though it is not straightforward to test that for the observed response. This is because the environment in this study is dynamically changing and hence the key parameters in the framework, such as the birth and death rate, dispersion, and so on of each OTU are not kept. And even if the effect of nutrition input is nicely modeled by the abrupt change in such parameters, to reproduce the responses in the later time remains as a difficult task.

Finally, present finding is also meaningful in the agricultural context. It is important in agriculture to put organic matter such as compost into the soil to maintain the quality of the soil. Fertilizers as well are basically essential for producing crops on agricultural field soil. And, giving carbon source and/or nitrogen source to soil in this way can be regarded as one of the disturbance of soil ecosystem. It was reported that fertilization had a greater effect on soil bacterial community structure than crop rotation and growth stage (Guo et al. 2020). It is also shown that soil organic carbon and total nitrogen are two of the major determinants of community composition (Li et al. 2017). The disturbance of the shape of the OTU-RSA curve for the soil amended with carbon and nitrogen sources (glucose and ammonium chloride, respectively) (Fig. 1) clearly indicate a rapid changes in bacterial community structure. In addition, when combined with traditional analyses such as non-metric multidimensional scaling (NMDS) (SI Fig. 4), the overall picture of the changes that occur in the community structure becomes easier to understand.

METHODS

Sample Preparation and Primary Sequence Analysis

Nucleotide sequence files registered in DDBJ/ENA/GenBank under the accession numbers DRR157393-157518 (DRA007564) and DRR169428-169475 (DRA008081) were retrieved. These sequences were generated by amplicon sequencing targeting 16S rRNA genes in soil microcosms amended with labile carbon and nitrogen sources (partly described in [36]). These genes are the commonly-used "marker" for the identification of prokaryotes. The soil microcosm incubation experiment was designed in a full-factorial manner: besides control samples without nutritional amendment, eight treatment groups, differing in carbon source (glucose or cellobiose), nitrogen source (ammonium chloride or urea), and timing(s) of nutritional amendment (weekly amendment over the experiment period or abrupt amendment of quadruple amount at the beginning of incubation), were prepared (Table 1). The total amount of carbon and nitrogen input was the same in all groups. Twelve microcosms were constructed for each group, three of which were destructively sampled after 3, 10, 17, and 24 days of incubation. Additionally, the pre-incubation (i.e. day 0) soil was examined in triplicate. Sampled soil was subjected to total DNA extraction, purification, amplification of partial 16S rRNA gene sequence, and Illumina high-throughput sequencing as described previously [36].

Low-quality (i.e. expected errors of 0.5 bases or more) sequences were removed using USEARCH v9.2.64 [40]. Subsequently singleton sequences were removed, and the remaining sequences were clustered into operational taxonomic units (OTUs) at a similarity threshold of 97% or more using UPARSE [41]. The OTU representative sequences (i.e. most frequently-observed sequence within those clustered into the OTU) were subjected to UCHIME2 [42] to filter out chimera-like OTUs. Finally, all the quality-filtered sequences, including singletons, were mapped to OTU representative sequences using USEARCH v9.2.64. To detect organelle-like OTUs, the OTU representative sequences were taxonomically annotated by RDP classifier [43] trained with Greengenes 13.8 clustered at 97% [44]. OTUs annotated as "family mitochondria" or "class Chloroplast" were precluded from further analyses.

Species Abundance Distributions

To characterize the SAD, we compare the fittings by log-normal distribution

$$P^{LN}(\mu, \sigma; x) = \frac{1}{\sigma x \sqrt{2\pi}} \exp \left\{ -\frac{(\ln x - \mu)^2}{2\sigma^2} \right\}, \quad (6)$$

power-law (Zipf/Pareto) distribution

$$P^{PL}(\alpha, \theta; x) = \frac{\alpha \theta^\alpha}{(x + \theta)^{\alpha+1}}, \quad (7)$$

and the negative binomial distribution

$$P^{NB}(s, p; x) = \frac{\Gamma(x + s)}{\Gamma(x + 1) \Gamma(s)} p^s (1 - p)^x, \quad (8)$$

where x denote the OTU abundance.

The obtained fitting parameter values; $\ln \mu \sim \ln \sigma \sim 1.5$ for the log-normal distribution, shape parameter $1.0 < \alpha < 1.5$ for Pareto distribution, and the size $0 < s < 0.75$ and the mean $p \sim 0.01$ for the negative binomial distribution, consistently indicate that the OTU-SAD of the soil microbe ecosystem before any artificial nutrition input is very broad, i.e. critical or fat-tailed (see SI for detail).

ACKNOWLEDGEMENT

TS was partly supported by JSPS KAKENHI grant number JP18K03449 and JP23K03256. TS and SO were partly supported by JSPS KAKENHI grant number JP17K19220. KMo was partly supported by JSPS KAKENHI Grant Number JP20K19885.

-
- [1] R. MacArthur, Fluctuations of animal populations and a measure of community stability, *Ecology* **36**, 533 (1955).
 - [2] M. R. Gardner and W. R. Ashby, Connectance of large dynamic (cybernetic) systems: critical values for stability, *Nature* **228**, 784 (1970).
 - [3] R. M. May, Will a large complex system be stable?, *Nature* **238**, 413 (1972).
 - [4] K. Tregonning and A. Roberts, Complex systems which evolve towards homeostasis, *Nature* **281**, 563 (1979).
 - [5] S. L. Pimm, Complexity and stability: another look at macarthur's original hypothesis, *OIKOS* **33**, 351 (1979).
 - [6] S. L. Pimm, The complexity and stability of ecosystems, *Nature* **307**, 321 (1984).
 - [7] P. J. Taylor, Consistent scaling and parameter choice for linear and generalized lotka-volterra models used in community ecology, *J. theor. Biol.* **135**, 543 (1988).
 - [8] K. S. McCann, The diversity-stability debate, *Nature* **405**, 228 (2000).
 - [9] M. Kondoh, Foraging adaptation and the relationship between food-web complexity and stability, *Science* **299**, 1388 (2003), <http://science.sciencemag.org/content/299/5611/1388.full.pdf>.
 - [10] C. Quince, P. G. Higgs, and A. J. McKane, Deleting species from model food webs, *OIKOS* **110**, 283 (2005).
 - [11] T. C. Ings, J. M. Montoya, J. Bascompte, N. Blüthgen, L. Brown, C. F. Dormann, F. Edwards, D. Figueroa, U. Jacob, J. I. Jones, R. B. Lauridsen, M. E. Ledger, H. M. Lewis, J. M. Olesen, F. F. Van Veen, P. H. Warren, and G. Woodward, Review: Ecological networks – beyond food webs, *Journal of Animal Ecology* **78**, 253 (2009).
 - [12] A. Mougi and M. Kondoh, Diversity of interaction types and ecological community stability, *Science* **337**, 349 (2012), <http://science.sciencemag.org/content/337/6092/349.full.pdf>.
 - [13] B. S. Griffiths and L. Philippot, Insights into the resistance and resilience of the soil microbial community, *FEMS Microbiology Reviews* **37**, 112 (2013).
 - [14] P. Bak and K. Sneppen, Punctuated equilibrium and criticality in a simple model of evolution, *Phys. Rev. Lett.* **71**, 4083 (1993).
 - [15] R. V. Solé and J. Bascompte, Are critical phenomena relevant to large-scale evolution?, *Proc. R. Soc. Lond. B* **263**, 161 (1996).
 - [16] K. Tokita and A. Yasutomi, Mass extinction in a dynamical system of evolution with variable dimension, *Phys. Rev. E* **60**, 842 (1999).
 - [17] R. Albert, H. Jeong, and A.-L. Barabási, Error and attack tolerance of complex networks, *Nature* **406**, 378 (2000).

- [18] S. Jain and S. Krishna, Large extinctions in an evolutionary model: The role of innovation and keystone species of innovation and keystone species, *Proc. Natl. Acad. Sci. USA* **99**, 2055 (2002).
- [19] K. Christensen, S. A. di Collobiano, M. Hall, and H. J. Jensen, Tangled nature: a model of evolutionary ecology, *J. theor. Biol.* **216**, 73 (2002).
- [20] S. V. Buldyrev, R. Parshani, G. Paul, H. E. Stanley, and S. Havlin, Catastrophic cascade of failures in interdependent networks, *Nature* **464**, 1025 (2010).
- [21] T. Shimada, A universal transition in the robustness of evolving open systems, *Scientific Reports* **4**, 4082 EP (2014).
- [22] F. Ogushi, J. Kertész, K. Kaski, and T. Shimada, Enhanced robustness of evolving open systems by the bidirectionality of interactions between elements, *Scientific Reports* **7**, 6978 (2017).
- [23] J. Trevors, One gram of soil: a microbial biochemical gene library, *Antonie Van Leeuwenhoek* **97**, 99 (2010).
- [24] T. P. Curtis, W. T. Sloan, and J. W. Scannell, Estimating prokaryotic diversity and its limits, *Proceedings of the National Academy of Sciences* **99**, 10494 (2002).
- [25] B. S. Griffiths and L. Philippot, Insights into the resistance and resilience of the soil microbial community, *FEMS microbiology reviews* **37**, 112 (2013).
- [26] W. Swenson, D. S. Wilson, and R. Elias, Artificial ecosystem selection, *Proceedings of the National Academy of Sciences* **97**, 9110 (2000) <https://www.pnas.org/content/97/16/9110.full.pdf>.
- [27] M. Hamady, J. J. Walker, J. K. Harris, N. J. Gold, and R. Knight, Error-correcting barcoded primers for pyrosequencing hundreds of samples in multiplex, *Nature Methods* **5**, 235 (2008).
- [28] J. G. Caporaso, C. L. Lauber, W. A. Walters, D. Berg-Lyons, J. Huntley, N. Fierer, S. M. Owens, J. Betley, L. Fraser, M. Bauer, N. Gormley, J. A. Gilbert, G. Smith, and R. Knight, Ultra-high-throughput microbial community analysis on the Illumina HiSeq and MiSeq platforms, *The ISME Journal* **6**, 1621 (2012).
- [29] K. M. Handley, K. C. Wrighton, C. S. Miller, M. J. Wilkins, R. S. Kantor, B. C. Thomas, K. H. Williams, J. A. Gilbert, P. E. Long, and J. F. Banfield, Disturbed subsurface microbial communities follow equivalent trajectories despite different structural starting points, *Environmental Microbiology* **17**, 622 (2015).
- [30] B. J. Ridenhour, S. L. Brooker, J. E. Williams, J. T. Van Leuven, A. W. Miller, M. D. Dearing, and C. H. Remien, Modeling time-series data from microbial communities, *The ISME Journal* **11**, 2526 (2017).
- [31] M. S. Samad, C. Johns, K. G. Richards, G. J. Lanigan, C. A. de Klein, T. J. Clough, and S. E. Morales, Response to nitrogen addition reveals metabolic and ecological strategies of soil bacteria, *Molecular Ecology* **26**, 5500 (2017).
- [32] S. D. Jurburg, I. Nunes, J. C. Stegen, X. Le Roux, A. Priemé, S. J. Sørensen, and J. F. Salles, Autogenic succession and deterministic recovery following disturbance in soil bacterial communities, *Scientific Reports* **7**, 1 (2017).
- [33] K. Faust, L. Lahti, D. Gonze, W. M. de Vos, and J. Raes, Metagenomics meets time series analysis: unraveling microbial community dynamics, *Current Opinion in Microbiology* **25**, 56 (2015).
- [34] W. R. Shoemaker, K. J. Locey, and J. T. Lennon, A macroecological theory of microbial biodiversity, *Nature Ecology & Evolution* **1**, 0107 (2017).
- [35] S. Marino, N. T. Baxter, G. B. Huffnagle, J. F. Petrosino, and P. D. Schloss, Mathematical modeling of primary succession of murine intestinal microbiota, *Proceedings of the National Academy of Sciences* **111**, 439 (2014), <https://www.pnas.org/content/111/1/439.full.pdf>.
- [36] K. Mise, R. Maruyama, Y. Miyabara, T. Kunito, K. Senoo, and S. Otsuka, Time-series analysis of phosphorus-depleted microbial communities in carbon/nitrogen-amended soils, *Applied Soil Ecology* **145**, 103346 (2020).
- [37] R. H. Whittaker, Vegetation of the siskiyou mountains, oregon and california, *Ecological monographs* **30**, 279 (1960).
- [38] J. R. Bray and J. T. Curtis, An ordination of the upland forest communities of southern wisconsin, *Ecological monographs* **27**, 326 (1957).
- [39] C. A. Lozupone, M. Hamady, S. T. Kelley, and R. Knight, Quantitative and qualitative β diversity measures lead to different insights into factors that structure microbial communities, *Applied and environmental microbiology* **73**, 1576 (2007).
- [40] R. C. Edgar, Search and clustering orders of magnitude faster than BLAST, *Bioinformatics* **26**, 2460 (2010), arXiv:Edgar, Robert C., 2010, Search.
- [41] R. C. Edgar, UPARSE: highly accurate OTU sequences from microbial amplicon reads, *Nature Methods* **10**, 996 (2013).
- [42] R. C. Edgar, UCHIME2: improved chimera prediction for amplicon sequencing, *bioRxiv*, 074252 (2016).
- [43] Q. Wang, G. M. Garrity, J. M. Tiedje, and J. R. Cole, Naive Bayesian classifier for rapid assignment of rRNA sequences into the new bacterial taxonomy, *Applied and Environmental Microbiology* **73**, 5261 (2007), arXiv:Wang, Qiong, 2007, Naive.
- [44] D. McDonald, M. N. Price, J. Goodrich, E. P. Nawrocki, T. Z. Desantis, A. Probst, G. L. Andersen, R. Knight, and P. Hugenholtz, An improved Greengenes taxonomy with explicit ranks for ecological and evolutionary analyses of bacteria and archaea, *The ISME Journal* **6**, 610 (2012).

SUPPLEMENTARY INFORMATION

NMDS

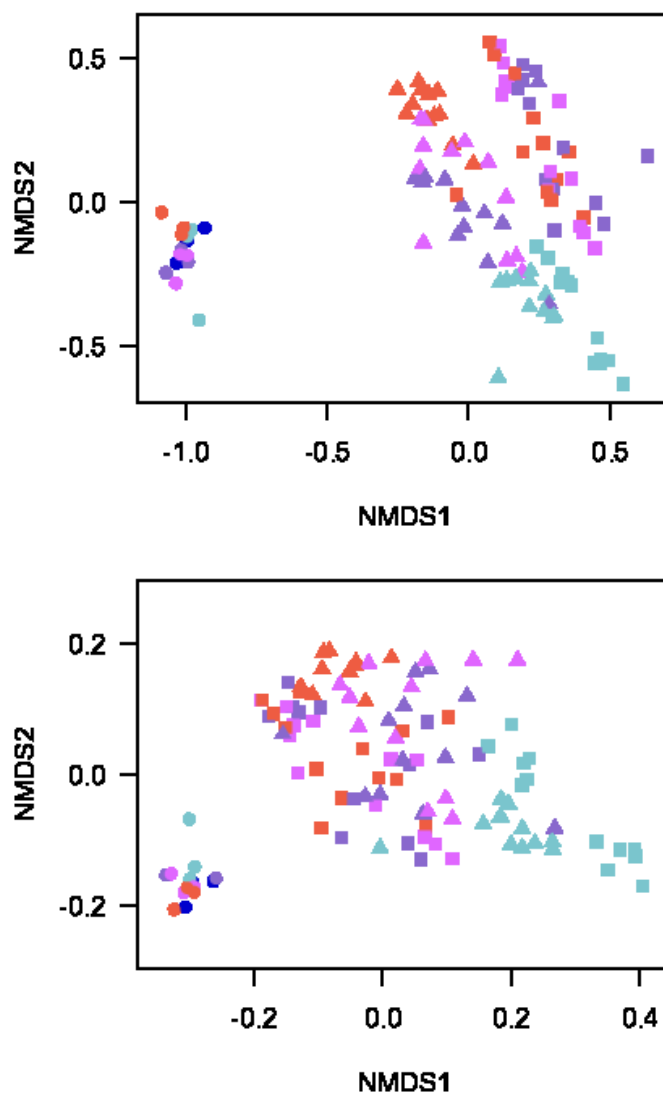


FIG. S-1. A non-metric dimensional scaling plot denoting the changes in microbial community compositions based on Bray-Curtis dissimilarities (upper) and weighted UniFrac distances (bottom). Circle, square, and triangle points denote no, abrupt, and weekly amendments of nutrients, respectively. Colors of the points corresponds to the stages (time after treatment): light blue, dark purple, light purple, and red represent the earliest, second earliest, third earliest, and the latest stages, respectively.

\mathcal{B} similarity to control soils

TABLE S-I. The average population-balance-based similarity $\bar{\mathcal{B}}$ to the control soils, with other characteristics relating to the diversity and RSA shape. \mathcal{B} similarity is defined as Eq. (2), with $R = 1,000$. The diversity and the dominance here represent the Shannon entropy of RSA: $S^\alpha = \sum_{r^\alpha} -p_r^\alpha \ln p_r^\alpha$ and the proportion of the sum of the abundances of top 10 OTUs to the total abundance, respectively.

Condition	Day	Diversity	Dominance	#OTU	$\bar{\mathcal{B}}^{100}$	$\bar{\mathcal{B}}^{1000}$	$\bar{\mathcal{C}}^{30}$	$\bar{\mathcal{C}}^{100}$	$\bar{\mathcal{C}}^{300}$
Control	0	6.741	0.128	4293	0.978	0.986	0.843	0.814	0.776
	3	6.648	0.146	3805	0.966	0.969	0.804	0.790	0.749
	10	6.689	0.124	3607	0.973	0.983	0.832	0.810	0.761
	17	6.692	0.124	3659	0.970	0.982	0.834	0.819	0.766
	24	6.823	0.112	4324	0.980	0.985	0.844	0.824	0.773
AG1	3	2.588	0.875	1696	0.700	0.580	0.258	0.332	0.437
	10	4.373	0.567	3080	0.756	0.664	0.224	0.042	0.230
	17	4.185	0.583	2761	0.721	0.623	0.157	0.031	0.223
	24	4.649	0.522	2861	0.793	0.708	0.175	0.064	0.257
AG4	3	4.032	0.625	3162	0.665	0.568	0.351	0.436	0.542
	10	4.814	0.476	3399	0.666	0.587	0.304	0.304	0.404
	17	3.985	0.595	2954	0.613	0.520	0.207	0.195	0.304
	24	4.655	0.526	2906	0.828	0.737	0.104	0.155	0.310
AC1	3	2.678	0.864	1867	0.728	0.601	0.230	0.349	0.428
	10	4.062	0.644	2600	0.833	0.727	0.089	0.069	0.272
	17	4.249	0.585	2540	0.796	0.702	0.043	-0.009	0.221
	24	4.429	0.543	2462	0.812	0.726	0.070	0.008	0.220
AC4	3	4.073	0.634	2897	0.697	0.592	0.353	0.494	0.588
	10	4.391	0.588	2856	0.804	0.697	0.119	0.277	0.460
	17	3.977	0.660	2665	0.814	0.699	0.048	0.153	0.325
	24	5.012	0.433	3032	0.804	0.737	-0.017	0.003	0.218
UG1	3	3.302	0.774	2034	0.764	0.644	0.159	0.295	0.424
	10	4.622	0.510	2475	0.877	0.794	0.080	-0.059	0.167
	17	4.786	0.469	2522	0.860	0.788	0.070	-0.086	0.143
	24	4.681	0.503	2668	0.820	0.736	0.085	0.058	0.227
UG4	3	3.792	0.682	2652	0.693	0.584	0.347	0.517	0.575
	10	4.073	0.638	2601	0.762	0.652	0.232	0.378	0.454
	17	4.417	0.556	2504	0.781	0.687	0.089	0.095	0.234
	24	5.155	0.407	2730	0.840	0.779	0.101	0.018	0.181
UC1	3	3.615	0.737	2325	0.765	0.650	0.174	0.340	0.433
	10	4.542	0.528	2501	0.853	0.767	0.007	-0.097	0.147
	17	4.909	0.447	2534	0.904	0.836	-0.012	-0.172	0.109
	24	4.958	0.434	2620	0.913	0.846	-0.016	-0.161	0.121
UC4	3	3.460	0.729	2582	0.670	0.559	0.295	0.501	0.547
	10	4.690	0.517	2863	0.835	0.745	0.038	0.101	0.285
	17	4.634	0.519	2518	0.798	0.710	-0.009	0.054	0.226
	24	4.828	0.465	2612	0.770	0.698	0.017	0.007	0.182

Similarity of the control soils in OTU composition

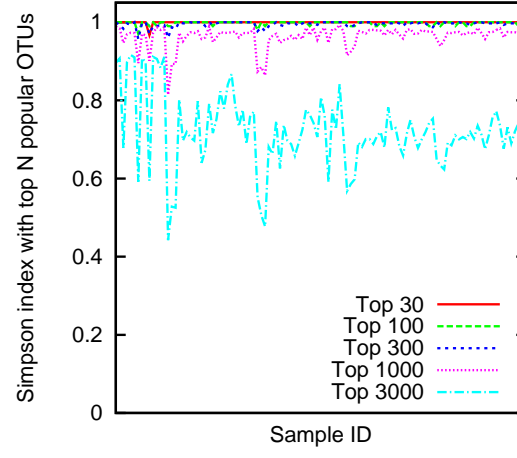


FIG. S-2. The overlap coefficient (Szymkiewicz-Simpson coefficient) $S_{\alpha\beta} \equiv \frac{|\alpha \cap \beta|}{\min(|\alpha|, |\beta|)}$ between the set of top N popular OTUs α and the OTUs in each soil β . Almost all of top 300 major OTUs are detected in all soils while some of top 1,000 popular OTUs are missing (i.e. absent or undetectable).

Characteristics of RSA distributions

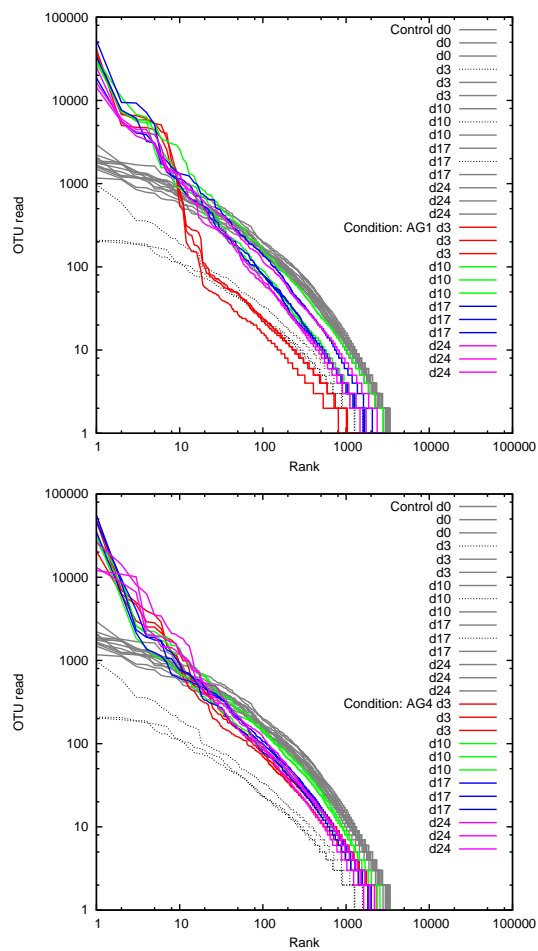


FIG. S-3. Rank-size distributions of OTUs under fertilization with Ammonium chloride and Glucose (Left: abrupt, Right: weekly 4 times).

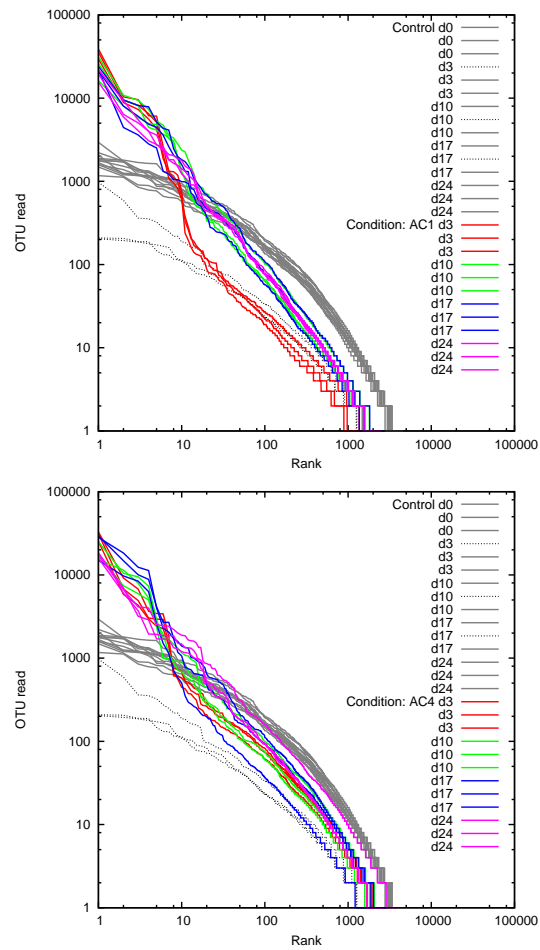


FIG. S-4. Rank-size distributions of OTUs under fertilization with Ammonium chloride and Cellobiose (Left: abrupt, Right: weekly 4 times).

TABLE S-II. Characteristics of the rank-size plots of control soils.

SampleID	Day	Diversity	Dominance	#OTU	tot. # _{read}
1	0	6.740	0.126	4246	97138
2	0	6.723	0.133	4213	79576
3	0	6.759	0.125	4421	87402
4	3	6.495	0.187	2696	20039
6	3	6.736	0.120	4441	105427
7	10	6.755	0.113	4304	90000
8	10	6.647	0.119	2123	12961
9	10	6.665	0.140	4395	92151
10	17	6.713	0.125	4514	113768
11	17	6.601	0.122	2124	13262
12	17	6.760	0.124	4341	87653
13	24	7.026	0.094	4602	83224
14	24	6.727	0.119	4023	73965
15	24	6.717	0.123	4347	88142

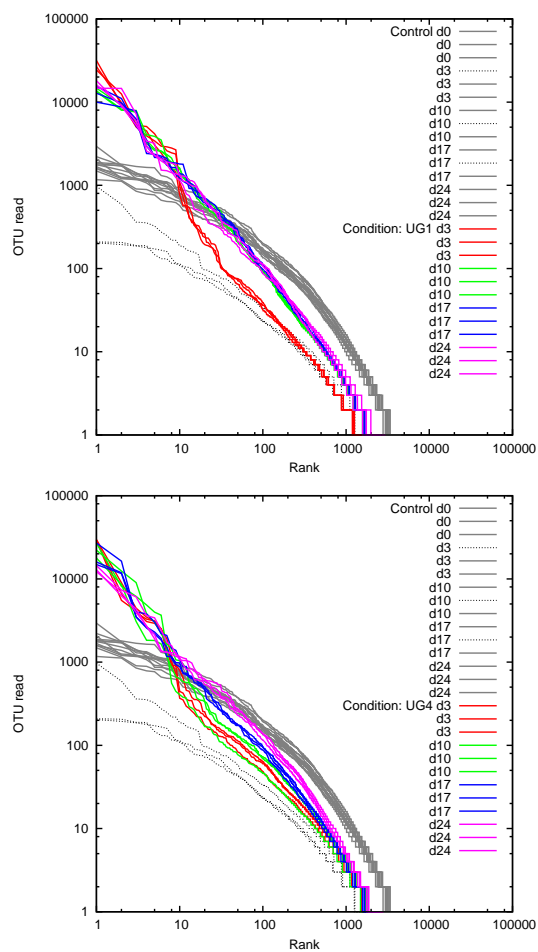


FIG. S-5. Rank-size distributions of OTUs under fertilization with Urea and Glucose (Left: abrupt, Right: weekly 4 times).

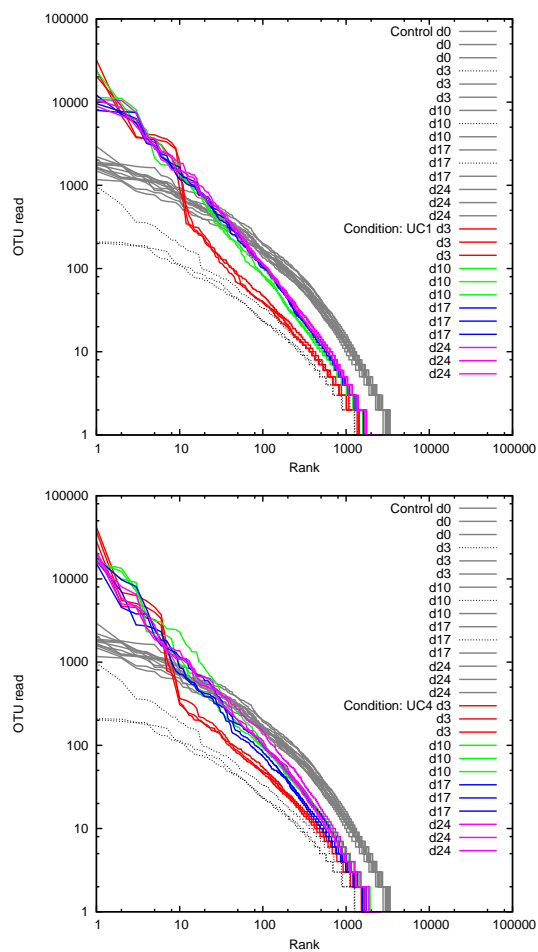


FIG. S-6. Rank-size distributions of OTUs under fertilization with Urea and Cellobiose (Left: abrupt, Right: weekly 4 times).

TABLE S-III. Characteristics of the rank-size plots of the soils with Ammonium chloride as the nitrogen source.

SampleID	Day	Diversity	Dominance	#OTU	tot.	#read
(AG1)	16	3	2.277	0.902	1479	77263
	17	3	2.790	0.857	1819	84824
	18	3	2.698	0.866	1791	86315
	19	10	5.071	0.464	3956	146007
	20	10	4.004	0.619	2615	94330
	21	10	4.043	0.619	2669	111668
	22	17	4.486	0.530	2548	79529
	23	17	3.988	0.619	2567	97617
	24	17	4.079	0.600	3170	152920
	25	24	4.075	0.605	2333	84754
	26	24	4.636	0.537	2740	69740
27	24	5.237	0.422	3511	98191	
(AG4)	28	3	4.807	0.515	3222	84241
	29	3	3.535	0.695	2933	103057
	30	3	3.753	0.664	3333	124647
	31	10	4.410	0.532	3053	86813
	32	10	5.019	0.451	3497	112981
	33	10	5.013	0.447	3647	122846
	34	17	4.020	0.599	3035	117447
	35	17	4.126	0.571	2816	87447
	36	17	3.809	0.615	3012	123010
	37	24	4.514	0.544	2541	81316
	38	24	4.404	0.571	2929	123503
39	24	5.049	0.464	3250	87409	
(AC1)	40	3	2.862	0.837	2288	84250
	41	3	2.557	0.879	1711	89076
	42	3	2.616	0.875	1604	70229
	43	10	4.196	0.633	2519	84433
	44	10	3.823	0.689	2418	95165
	45	10	4.165	0.610	2863	132677
	46	17	4.093	0.591	2250	69308
	47	17	4.379	0.572	2796	121407
	48	17	4.275	0.592	2574	95467
	49	24	4.666	0.494	2517	81237
	50	24	4.212	0.579	2348	94279
51	24	4.407	0.555	2523	84132	
(AC4)	52	3	4.077	0.633	2691	72891
	53	3	4.199	0.610	3037	91357
	54	3	3.942	0.659	2963	95568
	55	10	4.531	0.562	2810	75738
	56	10	4.153	0.636	2615	75640
	57	10	4.489	0.567	3145	110202
	58	17	3.997	0.660	2850	124981
	59	17	3.602	0.733	2117	63296
	60	17	4.333	0.586	3028	132373
	61	24	4.741	0.477	2635	84676
	62	24	5.466	0.364	3847	125750
63	24	4.829	0.458	2614	83179	

TABLE S-IV. Characteristics of the rank-size plots of the soils with Urea as the nitrogen source

	SampleID	Day	Diversity	Dominance	#OTU tot.	#read	
(UG1)	64	3	3.288	0.783	1968	78348	
	65	3	3.384	0.755	2018	76670	
	66	3	3.236	0.784	2116	85661	
	67	10	4.608	0.513	2456	87498	
	68	10	4.621	0.512	2480	93963	
	69	10	4.637	0.505	2491	91091	
	70	17	4.837	0.465	2530	90556	
	71	17	4.869	0.453	2463	89096	
	72	17	4.651	0.490	2573	95837	
	73	24	4.789	0.470	2629	96630	
	74	24	4.575	0.505	2406	91239	
	75	24	4.680	0.535	2971	91612	
	(UG4)	76	3	3.866	0.669	2714	78639
		77	3	3.861	0.674	2736	84624
		78	3	3.647	0.702	2506	72037
79		10	3.558	0.733	2398	77141	
80		10	4.519	0.545	2632	69803	
81		10	4.140	0.637	2775	90771	
82		17	4.604	0.535	2540	87544	
83		17	4.531	0.536	2410	76750	
84		17	4.116	0.599	2564	96683	
85		24	5.138	0.411	2603	82586	
86		24	5.218	0.386	2762	89540	
87		24	5.110	0.424	2826	101649	
(UC1)		88	3	3.848	0.700	2330	72345
		89	3	3.626	0.741	2357	75994
		90	3	3.370	0.771	2288	87739
	91	10	4.679	0.504	2516	83231	
	92	10	4.487	0.552	2437	89271	
	93	10	4.460	0.527	2550	102115	
	94	17	4.890	0.447	2509	90361	
	95	17	4.902	0.456	2549	87501	
	96	17	4.935	0.439	2545	87503	
	97	24	4.987	0.431	2634	96957	
	98	24	4.999	0.421	2558	87552	
	99	24	4.886	0.449	2670	103767	
	(UC4)	100	3	3.356	0.747	2656	96695
		101	3	3.618	0.704	2477	70112
		102	3	3.405	0.737	2614	84743
103		10	4.675	0.536	2888	88983	
104		10	4.763	0.511	2963	94337	
105		10	4.632	0.506	2739	110944	
106		17	4.645	0.517	2424	67638	
107		17	4.876	0.462	2649	85094	
108		17	4.382	0.578	2481	85904	
109		24	4.784	0.468	2619	91658	
110		24	4.970	0.438	2756	100208	
111		24	4.730	0.489	2461	85470	

Sample Accession ID

TABLE S-V. Sample Accession ID.

Condition	Day	Accession ID
Control	0	DRR157393-157395
C: none	3	DRR157396-157398
N: none	10	DRR157399-157401
timing: -	17	DRR157402-157404
	24	DRR157405-157407
AG1	3	DRR157408-157410
C: Glucose	10	DRR157411-157413
N: Ammonium chloride	17	DRR157414-157416
timing: Abrupt	24	DRR157417-157419
AG4	3	DRR157420-157422
C: Glucose	10	DRR157423-157425
N: Ammonium chloride	17	DRR157426-157428
timing: Weekly	24	DRR157429-157431
AC1	3	DRR157432-157434
C: Cellobiose	10	DRR157435-157437
N: Ammonium chloride	17	DRR157438-157440
timing: Abrupt	24	DRR157441-157443
AC4	3	DRR157444-157446
C: Cellobiose	10	DRR157447-157449
N: Ammonium chloride	17	DRR157450-157452
timing: Weekly	24	DRR157453-157455
UG1	3	DRR169428-169430
C: Glucose	10	DRR169431-169433
N: Urea	17	DRR169434-169436
timing: Abrupt	24	DRR169437-169439
UG4	3	DRR169440-169442
C: Glucose	10	DRR169443-169445
N: Urea	17	DRR169446-169448
timing: Weekly	24	DRR169449-169451
UC1	3	DRR169452-169454
C: Cellobiose	10	DRR169455-169457
N: Urea	17	DRR169458-169460
timing: Abrupt	24	DRR169461-169463
UC4	3	DRR169464-169466
C: Cellobiose	10	DRR169467-169469
N: Urea	17	DRR169470-169472
timing: Weekly	24	DRR169473-169475